ISSN 1063-7834, Physics of the Solid State, 2018, Vol. 60, No. 12, pp. 2358–2362. © Pleiades Publishing, Ltd., 2018.
Original Russian Text © A.D. Evstifeev, Yu.V. Petrov, N.A. Kazarinov, R.R. Valiev, 2018, published in Fizika Tverdogo Tela, 2018, Vol. 60, No. 12, pp. 2320–2324.

METALS

Strength of the Ti–6Al–4V Titanium Alloy under Conditions of Impact and Short Pulse Loading

A. D. Evstifeev[a, *], Yu. V. Petrov[a, b], N. A. Kazarinov[a], and R. R. Valiev[a, c]

[a] *St. Petersburg State University, St. Petersburg, 199034 Russia*
[b] *Institute of Problems of Mechanical Engineering, Russian Academy of Sciences, St. Petersburg, 199178 Russia*
[c] *Ufa State Aviation Technical University, Ufa, 450077 Russia*
**e-mail: ad.evstifeev@gmail.com*

Received May 11, 2018

Abstract—The strength and resistance of the Ti–6Al–4V titanium alloy to solid particle erosion have been studied in as-delivered state and after the equal-channel angular pressing. The ultrafine-grained material and the initial material have been tested for dynamic tension using an Instron drop tower testing machine and an aerodynamic setup for erosion testing with corundum particles as an abrasive material. Despite a substantial increase in the static strength properties, the ultrafine-grained material demonstrates the properties similar to those of the initial material under dynamic loads, which, in turn, has been analyzed based on a structural–temporal approach using the incubation time criterion.

DOI: 10.1134/S1063783418120120

1. INTRODUCTION

Tests of materials for applications in the aircraft industry include a certain number of experiments in quasi-static regimes and some special experiments aimed to reproduce operation conditions. For example, the tests of materials used in turbine blades of compressor engines include a series of erosion resistance experiments. The materials differ, as a rule, by the sample mass loss after tests with a given duration. In this case, the behavior of the materials under loads different from the model loads remains unstudied. Threshold characteristics of the external loading can be important parameters and the numerical analysis of the material properties using the methods and criteria of the dynamic fracture mechanics should be carried out [1].

Another aspect in the choice of a material for practical application is an opportunity of improving its strength and operation properties. One of the promising methods of changing material properties is the fabrication of an ultrafine-grained (UFG) structure using the severe plastic deformation method (SPD). This method is being studied all over the world [2]. The studies have been performed on the influence of the material structure evolution on the static strength [3], the plasticity, the fatigue strength [4], and the adhesion of protective coating [5]. The studies demonstrate the perspectivity of the SPD treatment for enhancement strength and operating properties of materials for practical application.

The increase in the strength and operating characteristics of the material subjected to extreme loads is impossible without experimental and theoretical studies of their dynamic strength properties. This report presents the results of studies of the titanium alloy Ti–6Al–4V used for fabrication of important structural elements in the aerospace industry [6, 7]. The strength and operation properties are analyzed using a structural–temporal approach in the fracture mechanics taking into account the material parameters obtained during the erosion and impact experiments.

2. MATERIALS

The microstructure of initial billets (20 mm in diameter) consisted of uniaxial α-phase grains with a mean size of 15 μm. To form a bimodal (mixed globular–lamellar) microstructure in the billets, the billets were subjected to a heat treatment (HT) including quenching from a temperature of 975°C into water with subsequent annealing at a temperature of 675°C for 4 h. To form the UFG structure, the initial billets were subjected to a combined deformation-thermal treatment. The equal-channel angular pressing (ECAP) [8–10] was carried out using the *Bc* route at which the blank was rotated by 90° around its longitudinal axis after each passage. During pressing at a temperature of 600°C, the material was pushed through two channels 20 mm in diameter intersecting at an

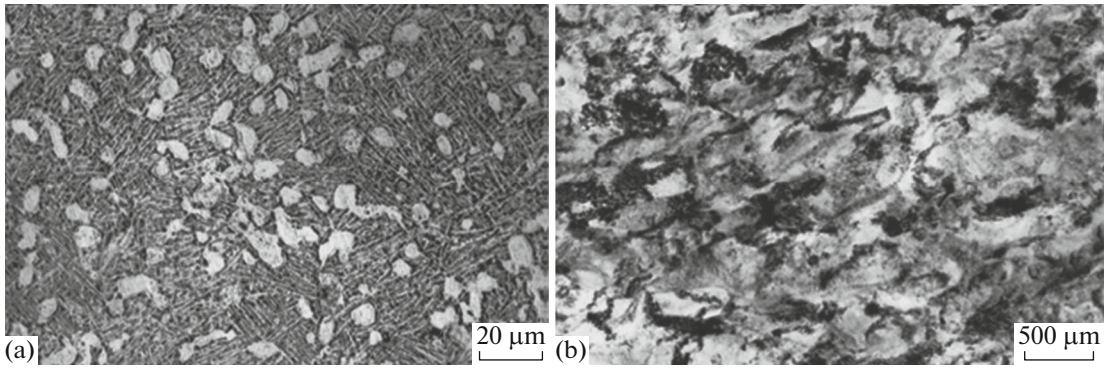

Fig. 1. Structures of the titanium alloy Ti–6Al–4V samples (a) in the initial and (b) the UFG states.

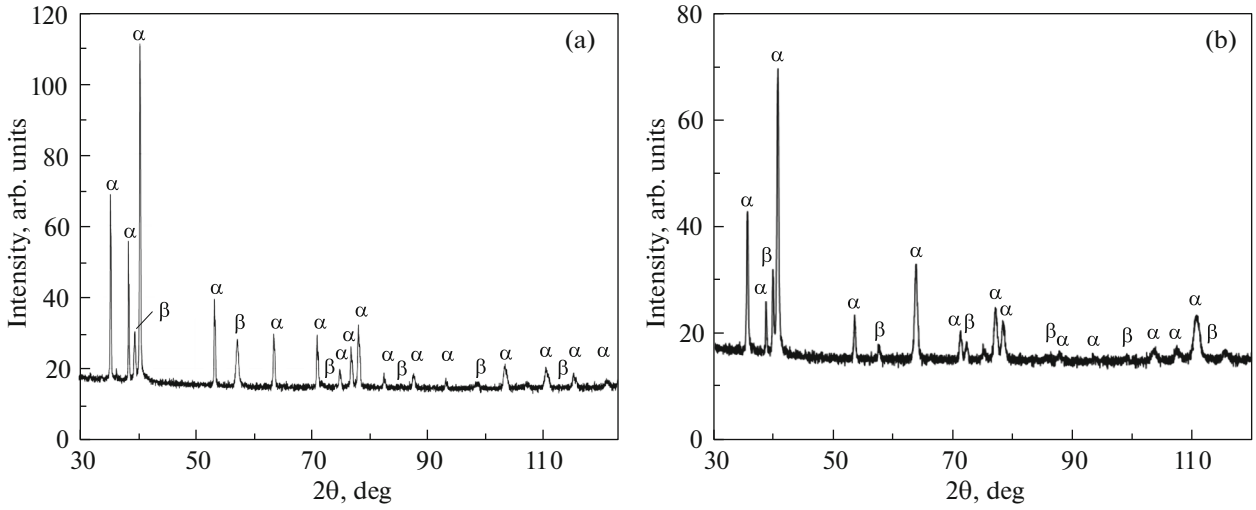

Fig. 2. X-ray diffraction patterns of the titanium alloy Ti–6Al–4V samples (a) in the initial and (b) the UFG states.

angle of 120°. The deformation stresses were removed by subsequent annealing at 500°C for 1 h.

Figure 1a shows the SEM image of the initial microstructure of the Ti–6Al–4V alloy. It can be seen that there are β-transformed lamellar structure with the mean grain size of the secondary phase 1 μm and the initial α-phase grain size about 8 μm whose volume fraction was not higher than 25%. Figure 1b demonstrates the typical UFG structure with the mean grain sizes of the α- and β-phases 250 nm formed in the Ti–6Al–4V alloy after ECAP treatment with subsequent annealing.

Figure 2 shows the typical X-ray diffraction of the titanium alloy in the initial and ultrafine-grained states.

The ECAP treatment led to the increase in the Vickers hardness by 11% from 321 ± 1.8 to 356 ± 3.8 HV. The short-time ultimate strength increases by 33% from 950 ± 30 MPa to 1200 ± 40 MPa.

3. THE TENSILE TEST TECHNIQUE AND THE RESULTS

The tensile tests were carried out using a Shimidzu AG-50kNX testing machine for tension in a quasi-static regime, and an Instron CEAST 9350 testing machine was used to realize impact tensile loads at a strain rate of 10^2–10^3 s^{-1}.

The geometric sizes of the specimens were chosen based on the microstructure features of the fabricated bulk nanostructured materials and the limitations on allowable load of the testing machines used. The specimen gauge part was 5 mm in length and 2 mm in width. The specimens were cut using an ARTA 123 PRO electroerosion machine and finished on a polishing wheel up to the same roughness parameters. The technique of experimental tensile tests using a tower testing machine was described in detail in [11, 12].

Figure 3 shows the extreme values of the maximum stresses for the studied materials as functions of the

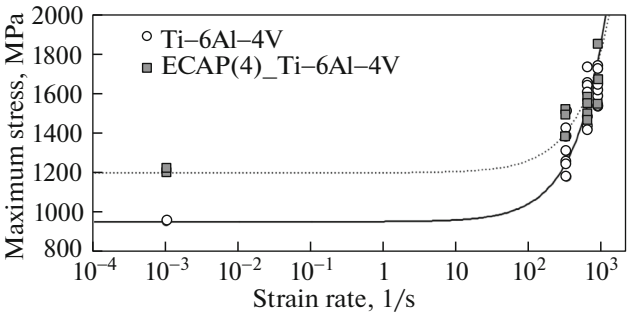

Fig. 3. Dependence of the tensile strength on the strain rate for Ti–6Al–4V samples in the initial and the UFG states. The dynamic strength curves were built using criterion (1) with the material parameters $E = 115$ GPa, $\tau_c = 16$ μs, and $\sigma_c = 950$ MPa for the initial alloy and $E = 115$ GPa, $\tau_c = 10$ μs, and $\sigma_c = 1200$ MPa for the UFG alloy.

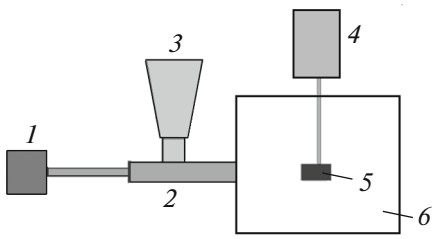

Fig. 4. Scheme of erosion setup: (*1*) compressor chamber, (*2*) accelerating channel, (*3*) solid phase disperser, (*4*) pneumatic drive for introducing the sample, (*5*) sample, and (*6*) working chamber.

strain rate. The results demonstrate that, under quasi-static loads, the alloy in the initial state has a lower strength than the alloy in the ultrafine-grained state. The difference between the materials decreases as the strain rate increases, and both materials demonstrate equal strength characteristics.

The features of the behavior of the material at high strain rates can be explained using the structural–temporal approach. We choose the incubation time criterion as a criterion of tensile fracture of the material [13, 14]:

$$\frac{1}{\tau_c}\int\limits_{t-\tau_c}^{t}\frac{\sigma(s)}{\sigma_c}ds \le 1, \qquad (1)$$

where t is the time, σ is the time dependence of the tensile stress, σ_c is the static tensile ultimate strength, and τ_c is the incubation fracture time that is the measure of strength in a dynamic range of external parameters. Constants σ_c and τ_c are the material parameters. In order to model tensile stress, we choose the stress that linearly increases in time, which is the closest to the experiment conditions.

We used the incubation time criterion and the experimental data and determined the material parameters $E = 115$ GPa, $\tau_c = 16$ μs, and $\sigma_c = 950$ MPa for the initial alloy and $E = 115$ GPa, $\tau_c = 10$ μs, and $\sigma_c = 1200$ MPa for the UFG alloy. Figure 3 shows the strain rate dependences which were built taking into account the material parameters. It is seen that the maximum tensile stresses increase nonlinearly with the strain rate. In this case, the experimental data in the dynamic range of the loading parameters can be explained by a decrease in the incubation time parameter that is responsible for the dynamic strength. Some authors explain the decrease in the dynamic strength of the titanium alloy Ti–6Al–4V after ECAP by the decrease in the plastic properties of the material due to the formation of a complex structure with high dislocation density and the internal stresses [15], which is also confirmed by the increase in the internal microdistortions of the crystal lattice determined by X-ray diffraction.

The numerical analysis of the experimental tensile tests of the titanium alloys in two states allow us to conclude that the strength characteristics of the titanium alloy Ti–6Al–4V (after ECAP) under the quasi-static loading conditions increase with the conservation of the strength properties in the dynamic loading range. In the framework of the aircraft industry, the results can become principally important when choosing materials for important dynamically loaded parts. The results of the abovementioned tests can be effectively used to predict fractures that accompany the erosion process [16]. For example, the behavior of the UFG titanium alloy Ti–6Al–4V in the operation conditions of compressor blades of turbine engines can be considered. The turbine blades are known to undergo high-speed erosion from dust particles. In this case, it should be noted that an erosion is essentially a dynamic load, since impacts of small particles lead to short-time pulses acting on the material surface.

4. EROSION TEST TECHNIQUE AND THE RESULTS

The Ti–6Al–4V alloy samples in the initial and the ultrafine-grained states were tested in pairs under the conditions of erosion flows for two powders with the mean fraction sizes 109 and 230 μm, respectively. The tests were carried at a constant concentration of solid particles in the flow of 1.7 g/s. Each pair of the samples was tested for 5 min. Figure 4 shows the experimental diagram [17] of the aerodynamic setup.

The change in the sample mass (Fig. 5) and the surface roughness (Fig. 6) were used as the parameters responsible for the fracture. The surface roughness was measured by a Surftest sj-210 profilometer with automatic calculation of the mean arithmetic deviation of the roughness profile points from the mean line (Ra).

The results of the erosion experiments demonstrate similar properties of the titanium alloy Ti–6Al–4V in

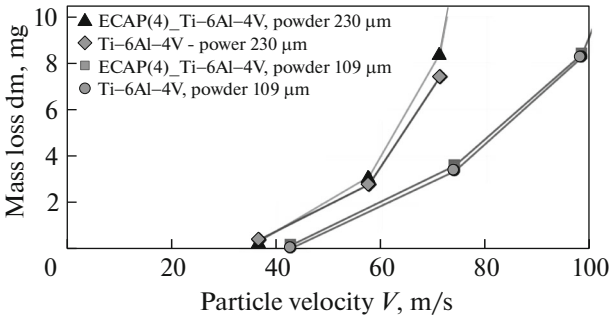

Fig. 5. Mass change of the titanium alloy Ti–6Al–4V samples in the initial and the UFG states (after ECAP) after the erosion test with the solid fraction sizes in an air flow 109 and 230 μm, respectively.

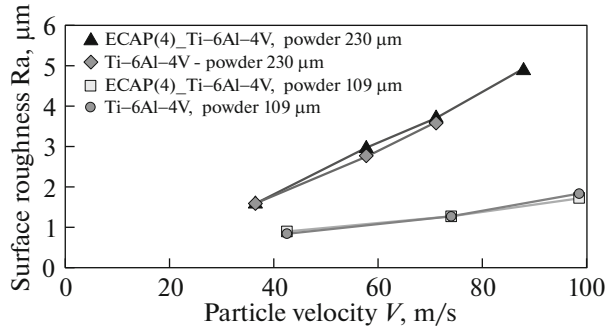

Fig. 6. Surface roughness of the titanium alloy Ti–6Al–4V samples in the initial and the UFG states after the erosion test with the solid fraction sizes in an air flow 109 and 230 μm, respectively.

the initial and the UFG states. Because the particle impacts on the surface act as high-speed pulses similar to dynamic loads, we can correlate these data with the data on the behavior of the materials under conditions of dynamic tensile loads. Thus, the erosion resistance of the material under conditions of high-rate pulse loads can be explained by the dynamic strength of the material.

We can note the increased strength and good operation characteristics of the titanium alloy Ti–6Al–4V after ECAP SPD treatment related to the conservation of the erosion resistance of the new material.

5. CONCLUSIONS

Using the structural–temporal approach and the results of the performed tensile experiments, we showed that the rate dependence of the strength has two branches responsible for the material behavior under conditions of static and dynamic loads. In the static deformation regimes, the UFG material demonstrated the strength that is 33% higher than the strength of the initial material. In this case, the discrepancies between the two materials became smaller as the strain rate increased. From the point of view of the structural–temporal approach, this can be explained by the decrease in the incubation time parameter during the SPD treatment. The decrease in the plastic properties of the material is related to the formation of a new structure in the material with a high dislocation density and internal stresses.

The studies carried out in this work showed that it is possible to increase the strength characteristics of the titanium alloy Ti–6Al–4V by SPD methods under conditions of quasi-static loads with the conservation of sufficient strength under dynamic conditions. This fact can be experimentally confirmed under conditions of dynamic tension and high-speed erosion. It should be noted as well that the development and introduction of new materials require the experimental and theoretical study of the strength and operation properties of materials in a wide range of external loading parameters.

ACKNOWLEDGMENTS

This work was supported by the Russian Science Foundation (no. 17-79-10145). N.A. Kazarinov and R.R. Valiev are grateful to the project of the Enterprise 3 of SPbGU (id: 26130576) for preparation of Section 2. The experimental studies were carried out using the equipment of the laboratory "Mechanics of advanced bulk nanomaterials for innovation engineering applications," of SPbGU, the Resource Centers of Scientific Park of SPbGU "Investigation of extreme states of materials and constructions" and "X-ray diffraction methods of studies."

REFERENCES

1. Yu. V. Petrov and V. I. Smirnov, Tech. Phys. **55**, 230 (2010).
2. R. Valiev, Nat. Mater. **3**, 511 (2004).
3. Q. Wei, H. T. Zhang, B. E. Schuster, K. T. Ramesh, R. Z. Valiev, L. J. Kecskes, R. J. Dowding, L. Magness, and K. Cho, Acta Mater. **54**, 4079 (2006).
4. Y. Estrin and A. Vinogradov, Int. J. Fatigue **32**, 898 (2010).
5. C. T. Wang, N. Gao, M. G. Gee, R. J. Wood, and T. G. Langdon, J. Mater. Sci. **48**, 4742 (2013).
6. M. Peters, J. Kumpfert, C. H. Ward, and C. Leyens, Adv. Eng. Mater. **5**, 419 (2003).
7. G. Welsch, R. Boyer, and E. W. Collings, *Materials Properties Handbook: Titanium Alloys* (ASM Int., Materials Park, OH, 1994).
8. R. Z. Valiev, R. K. Islamgaliev, and I. V. Alexandrov, Progr. Mater. Sci. **45**, 103 (2000).

9. I. P. Semenova, M. K. Smyslova, K. S. Selivanov, R. R. Valiev, and Y. M. Modina, IOP Conf. Ser.: Mater. Sci. Eng. 194, 012035 (2017).
10. I. P. Semenova, A. V. Polyakov, V. V. Polyakova, Y. Huang, R. Z. Valiev, and T. G. Langdon, Adv. Eng. Mater. **18**, 2057 (2016).
11. A. D. Evstifeev, A. A. Chevrychkina, and Y. V. Petrov, Mater. Phys. Mech. **32**, 258 (2017).
12. A. D. Evstifeev, J. Phys.: Conf. Ser. **991**, 012019 (2018).
13. Y. V. Petrov and A. A. Utkin, Sov. Mater. Sci. **25**, 153 (1989).
14. Y. V. Petrov and N. F. Morozov, ASME J. Appl. Mech. **61**, 710 (1994).
15. L. R. Saitova, I. P. Semenova, and I. V. Aleksandrov, Vestn. Samar. Tekh. Univ., Ser.: Fiz.-Mat. Nauki **27**, 164 (2004).
16. Y. V. Petrov, A. M. Bragov, N. A. Kazarinov, and A. D. Evstifeev, Phys. Solid State **59**, 93 (2017).
17. A. Evstifeev, N. Kazarinov, Y. Petrov, L. Witek, and A. Bednarz, Eng. Failure Anal. **87**, 15 (2018).

Translated by Yu. Ryzhkov